



BUDAPEST UNIVERSITY OF TECHNOLOGY AND ECONOMICS

Department of Morphology and Geometric Modeling

THE TIME EVOLUTION OF CRACK  
NETWORKS,  
*or, the Gilbert-piaffe*

Gergő Almádi  
Eszter Ferencz

Advisors:

Dr. Gábor Domokos

Dr. Ferenc Kun

HUN-REN BME Morphodynamics Research Group

TUDOMÁNYOS DIÁKKÖRI KONFERENCIA 2023

ANNUAL SCIENTIFIC STUDENT ASSOCIATION'S CONFERENCE 2023

**ABSTRACT.**

While in everyday life we often encounter the phenomena of cracking, it is very difficult either to control these processes or predict their potential occurrence. Since a fracturing process is an irreversible phenomenon and the formation of any new crack depends on the previously formed crack network, it is essential to study the development of fracture patterns as temporal processes to gain a deeper understanding of the phenomenon. Despite of how fundamental this question may seem, the literature has only recently begun to address its description. One of the most significant experiments conducted on this area was documented by Nakahara and his co-authors in 2018 [1].

The first step towards the mathematical description of fracturing processes is the (static) geometric description of crack patterns. The geometric model presented in the publications [2; 3] and illustrated with examples in the publication [4] summarizes the previous results in this field, putting them into a unified framework using the theory of convex mosaics. Within this model, a crack network can be identified with a *symbolic point* of the so-called *symbolic plane*, spanned by the network's two characteristic combinatorial averages  $\bar{n}^*, \bar{v}^*$ . Building on this model, we may ask the following question: if a crack network evolves over time due to various physical processes, how can the motion of its symbolic point be described based on knowledge of these physical processes? This question is raised in article [5] and answered in article [6]. The latter presents a general system of ordinary differential equations that can be applied to a wide range of cracking processes, after defining a so-called fundamental table which describes the physics of the specific process.

In our work we set up a model-hypothesis that the mosaic observed in experiment [1] is combinatorially equivalent to a convex mosaic, specifically the Gilbert mosaic. The Gilbert mosaic is a mathematical model in which cracks start from randomly chosen points on the plane and subsequently propagate in two opposite directions at uniform speed along a line defined by a randomly chosen angle until they reach another crack, where they stop at a so-called irregular ("T") node of degree  $n^* = 2$ .

We identified the fundamental table describing the evolution of the Gilbert mosaic and used it to define the model-specific version of the general equation presented in the article [4]. The model-specific system has one global attractor at  $(\bar{n}^*, \bar{v}^*) = (2, 4)$ . The evolution of the Gilbert mosaic inherently carries one of the most interesting phenomena observed in the experiment, namely that it only generates irregular nodes with the degree  $n^* = 2$ . Since  $n^* = 2$  is true only for a single point in the domain of convex mosaics on the symbolic plane, we can conclude that the time evolution of the Gilbert mosaic on the symbolic plane is a stationary process („piaffe"), as the mosaic's position on the plane will differ from the fixed point only because of the finite size of the mosaic.

Since the theory in [4] deals with the time evolution of infinite mosaics, we developed a numerical model that operates on finite mosaics for the purpose of precisely matching the experiment. The model has two important free parameters: the time delay between the initiation of each crack and the interval allowed for the random angle determining the line. By choosing these two parameters appropriately, we have achieved that the time evolution of the Gilbert mosaic reproduces not only the average cell number  $\bar{v}^*$  measured in the experimental mosaic, but also the evolution of the total cell degree distribution with surprising accuracy.

To our knowledge, this is the first time that a dynamic geometric model based on convex mosaics has been used to describe the evolution of a physical crack network.

**TABLE OF CONTENTS.**

ABSTRACT.....2

TABLE OF CONTENTS.....3

THE EXPERIMENT.....4

THEORY OF CONVEX MOSAICS.....5

    THE PIAFFE ON THE PLANE.....7

    THE GILBERT-PIAFFE.....10

NUMERIC MODEL.....11

RESULTS.....14

CONCLUSION.....16

LITERATURE.....17

## THE EXPERIMENT.

Understanding the processes and conditions required for the formation of crack patterns can be an important advance in many fields. A significant step in this area was a series of experiments carried out by Akio Nakahara and his colleagues: Tomoki Hiraoka, Rokuya Hayashi, Yousuke Matsuo and So Kitsunozaki in 2018 [1], which investigated whether the pattern of cracks caused by desiccation was affected by previous effects on the material. They suspected that a densely packed colloidal suspension (called a *paste*), can remember the direction of the vibrational motions or flow motions it has experienced before.

During the experiment, a mixture of colloidal particles of calcium carbonate (or magnesium carbonate) and water, which behaved as a plastic fluid, was created and poured into a container. After that, the mixture was dried at room temperature, the paste shrunk and stuck to the bottom of the container and the water evaporated, forming a characteristic desiccation pattern on the paste. Then it was examined whether samples exposed to different effects before the drying process gave different results in these patterns.

The study shows that when a paste experiences vibrational motion, all primary desiccation cracks propagate in the direction perpendicular to the direction of the vibrational motion. However, when a paste remembers a flow motion, all primary cracks spread along the flow direction (see Figure 1).

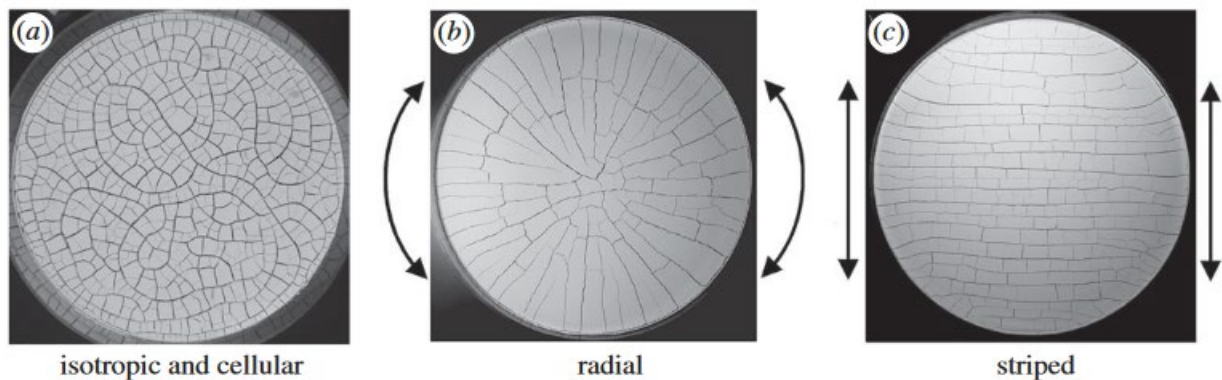


**Figure 1.** [1] The crack network of the paste when it experienced no motion before is isotropic and cellular (a). When a paste experiences vibrational motion, all primary desiccation cracks propagate in the direction perpendicular to the direction of the vibrational motion, causing the evolution of radial (b) and striped (c) networks.

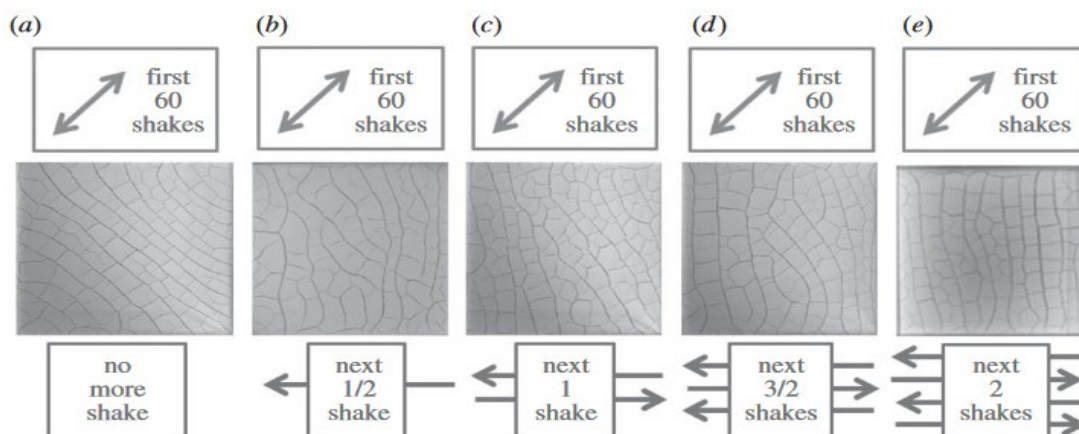


**Figure 2.** [1] Two additional vibrations are sufficient to overwrite old memory with new memory throughout the system (e). If the duration of the vibration is less than 2 shakes, the primary memory is only replaced in the rear region (a-d).

Furthermore, they also experimented with rewriting the memory of the paste by applying additional vibration to the paste along a different direction before the paste was fully dried [1].

Results show that two additional vibrations are sufficient to overwrite old memory with new memory throughout the system. However, if the duration of the additional vibration is less than two shakes, the primary vibration's memory is only replaced by the additional vibration's memory in the rear region (see Figure 2).

The results of these experiments were significant for our work because they provided us with well-documented data on the entire time evolution of a physical crack network. In the remainder of this paper, we will focus in more detail on the first experiment in the series, analysing the temporal variation of the mosaic pattern using the theory of convex mosaics.

## THEORY OF CONVEX MOSAICS.

To approach (static) crack networks mathematically, we have to introduce measures that can characterize a 2-dimensional convex tessellation (either created artificially or by natural fragmentation). Fortunately, the framework we use had already been established [39 in Plato], so we only introduce here the parameters, that are generally used to describe mosaics, based on [4]. Convex tessellations are coverings of the plane by convex polygons, without any gaps and any overlaps. We call the polygons the *cells* of the mosaic and we call points *nodes* where several vertices overlap. The number of vertices of a polygon is called the cell degree and denoted by  $v^*$  and the number of overlapping vertices at a node is called the nodal degree and denoted by  $n^*$ . The respective averages are denoted by  $\bar{n}^*$ ,  $\bar{v}^*$ . These two parameters span a plane  $[\bar{n}^*, \bar{v}^*]$  that is called the *symbolic plane* and a mosaic can be represented by one *symbolic point* on the plane.

Two major kinds of nodes exist in mosaics: regular and irregular ones. We call a node regular if only vertices of cells meet in that node. Most common regular nodes look like an “X” or a “Y” junction and have a (local) nodal degree of  $n^* = 4$  and  $n^* = 3$  respectively. A node is irregular if  $k$  vertices meet at one edge of a cell. The most common irregular node is a “T”-like junction, with a nodal degree of  $n^* = 2$ . In this paper we only deal with irregular T-nodes.

Based on the number of regular nodes ( $N_R$ ) and the number of irregular nodes ( $N_I$ ), following [2], we can define the *regularity* of the mosaic, as a third characteristic parameter with the following formula:

$$(1) \quad 0 \leq r \equiv N_R / (N_R + N_I) \leq 1.$$

The domain where convex mosaics exist on the symbolic plane had also been clarified [4]. It can be easily perceived if we look at the following formula:

$$(2) \quad \bar{v}^* = \frac{2\bar{n}^*}{(\bar{n}^* - r - 1)}$$

To specify the domain of convex mosaics in the symbolic plane, beyond equation (2), we also have to consider that the minimal degree of regular nodes and cells is three, while the minimal degree of irregular nodes is two (see Figure 3(a))

Beyond the  $[\bar{n}^*, \bar{v}^*]$  symbolic plane, the  $[x, y]$  *inverse symbolic plane* (see Figure 3) also has significance. These variables are defined as:

$$(3) \quad x = \frac{1}{\bar{n}^*},$$

$$(4) \quad y = \frac{1}{\bar{v}^*}$$

The domain of convex mosaics in the inverse symbolic plane is a quadrangle (see Figure 3(b)).

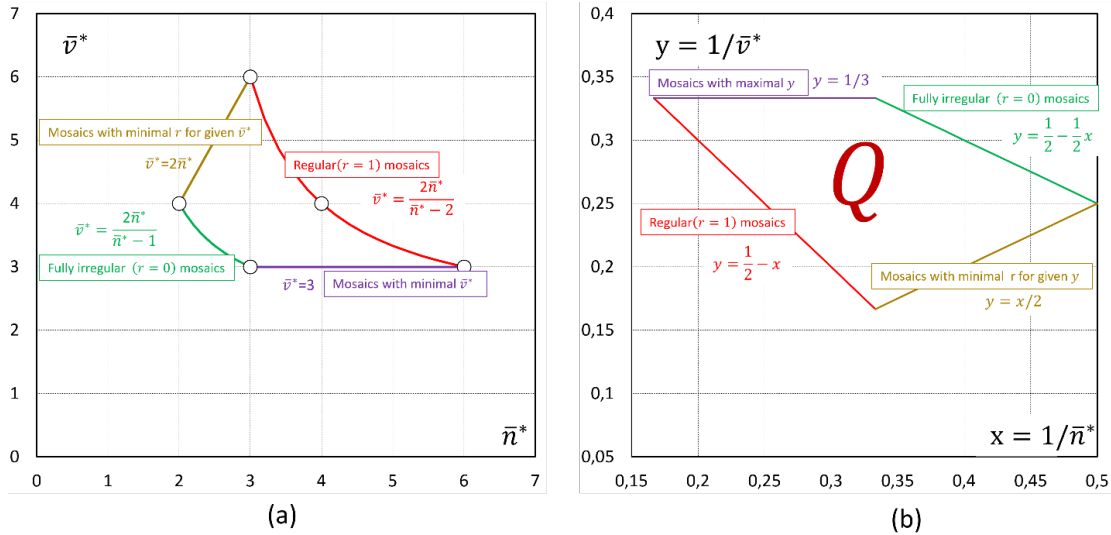


**Figure 3.** The symbolic plane (a) and the inverse symbolic plane (b). A mosaic can be represented by one symbolic point on both planes.

As a crack network evolves in time, the cell degree and nodal degree changes. In other words, the symbolic point representing a convex mosaic is moving along a trajectory on the symbolic plane and we may ask what sort of trajectories can come into existence? In [5] some rules had been stated for a discrete time evolution model, while in [6] a more general model is shown to track the movement of symbolic points in continuous time. Although the model in [6] develops ordinary differential equations (ODEs), the evolution is driven by a set of discrete cracking “micro” events in infinite mosaics.

The model in [6] bridges the gap between the discrete events and the evolution in continuous time. To derive the specific system of ODEs characterizing the evolution driven by one particular set of micro-events, a new tool is introduced in [6] and it is called the *fundamental table* (for one example, see Table 1). The fundamental table contains all the information on the micro events that can occur during the examined fragmentation. Such micro events may be secondary cracking, (when a new crack appears between two edges, so two new “T” junctions are created), or crack healing (when a “T” junction turns into a “Y” junction) (see Figure 4). The fundamental table also describes how each step is acting on the *fundamental variables*. These variables are the following:

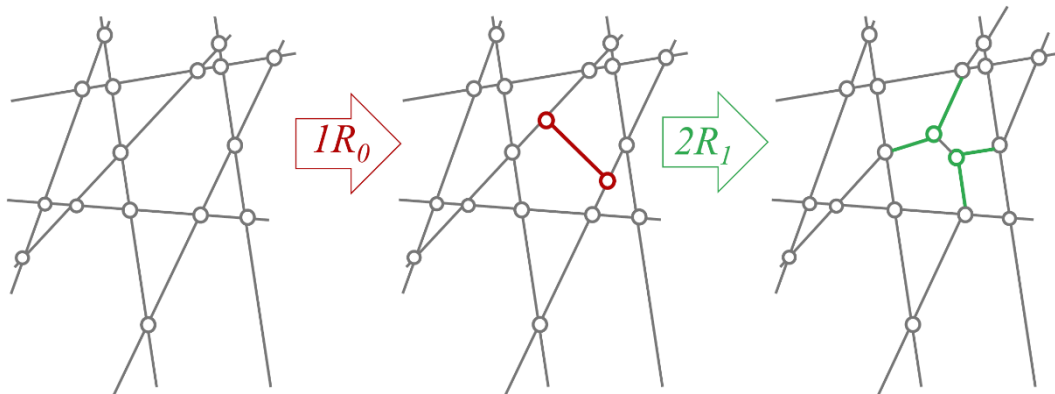


**Figure 4.** [6] Illustration of micro-events.  $R_0$ : secondary cracking, when two new “T” junctions appear.  $R_1$ : crack healing: when a “T” junction turns into a “Y” junction. (In the figure  $2R_1$  events are shown).

- $F$ : the number of faces (cells)
- $V$ : the number of vertices (nodes)

$N$ : the number of sharp corners.

Note that the authors in [6] assign likelihoods to the occurrences of each micro event, more precisely, these events are modelled as cumulative, discrete time random (Poisson) processes and the parameters of these processes (determining their intensities) are also included in the fundamental table  $(C_i, \lambda, q)$

It is demonstrated in [6], how for a fundamental table (describing a legit cracking process), a system of differential equations can be created. The solutions of these differential equations provide the trajectories that show the movement of a mosaic's symbolic point on the symbolic plane.

$i$	Name of step $R_i$	$C_{i,0}$	$C_{i,1}$	$C_{i,2}$	$\lambda_i$	$\Delta N(i)$	$\Delta V(i)$	$\Delta F(i)$
0	Secondary crack	1	0	0	$1 - q$	4	2	1
1	Crack healing	1	0	0	$q$	1	0	0

**Table 1.** [6] The fundamental table for the model used in [5] and illustrated in Figure 4.

### THE PIAFFE ON THE PLANE.

One might rather be astonished about a technical term from the noble world of dressage<sup>1</sup> in a mathematical paper. Piaffe is a movement in which the horse (and the rider) executes a slow elevated trot *on the spot*. In the following, we are going to discuss the properties of crack networks that throughout their evolution in time stay on the spot in the symbolic plane. We hope that this metaphor makes sense both for horse-lovers and for non-horse-lovers.

Take a look at a few examples:

**I.** First, let us consider an example moving within a finite frame, with its boundary being a regular square; this will be the first cell of the mosaic. The general step (which we will call step  $R_2$ ) that will describe the mosaic's temporal changes, or in other words the micro event applied in this example will be selecting an arbitrary interior point within any cell and connecting it with tree vertices of the cell in such a manner that all new cells

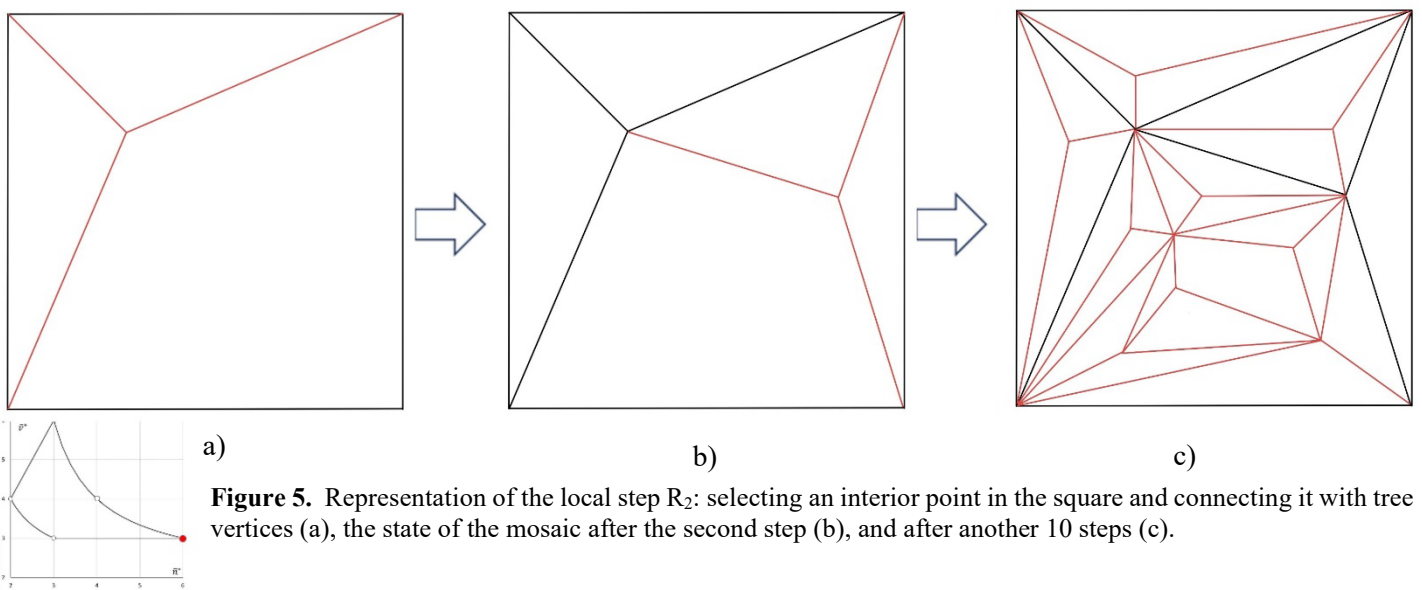


**Figure 5.** Representation of the local step  $R_2$ : selecting an interior point in the square and connecting it with tree vertices (a), the state of the mosaic after the second step (b), and after another 10 steps (c).

<sup>1</sup> “the training of a horse to perform special, carefully controlled movements as directed by the rider, or the performance of these movements as a sport or in a competition” [Cambridge Dictionary]

remain convex. The first step is illustrated in Figure 5(a) and the second in Figure 5(b). We can also identify the fundamental table of this process (Table 2) with the corresponding increments for the fundamental variables:  $\Delta F = 2, \Delta V = 1, \Delta N = 6$ . The first three entries of the table express the fact that on each cell we have exactly one exponential clock, triggering the discrete step. It can be observed that as the mosaic evolves over time (see Figure 5(c)), predominantly triangular cells are formed.

i	Name of step	$C_{i,0}$	$C_{i,1}$	$C_{i,2}$	$\lambda_i$	$\Delta N(i)$	$\Delta V(i)$	$\Delta F(i)$
2	3-way crack	1	0	0	1	6	1	2

**Table 2.** The fundamental table of the model illustrated in Figure 5.

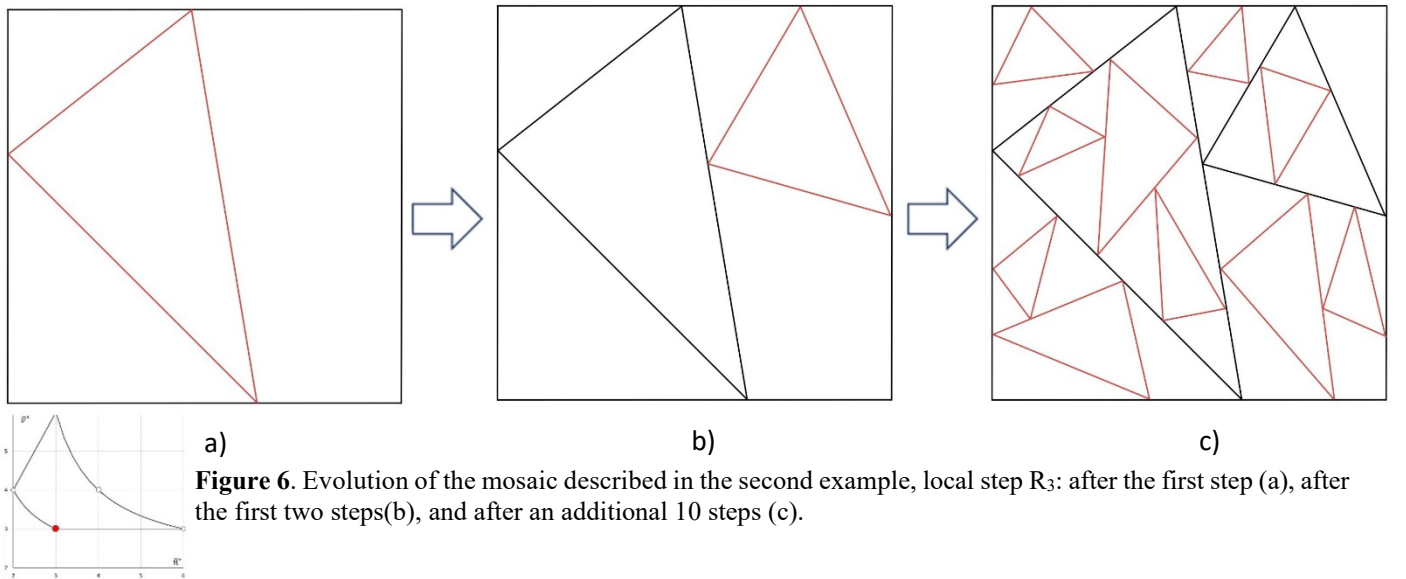
The algorithm described in article [6] allows us to define a model-specific version of the general differential equation system:

$$(5) \quad \frac{dx}{dt} = \lambda_0 y(1 - 6x)$$

$$(6) \quad \frac{dy}{dt} = 2\lambda_0 y(1 - 3y)$$

and we can see, we have  $x \rightarrow \frac{1}{6}$  and  $y \rightarrow \frac{1}{3}$  as  $t \rightarrow \infty$  which, via equations (3) and (4) also implies that  $\bar{n}^* \rightarrow 6$  and  $\bar{v}^* \rightarrow 3$  as  $t \rightarrow \infty$ .

**II.** For the second instance, we can create a mosaic similar to the previous one, utilizing a different micro event (which we will call step  $R_3$ ). Let us start again from the same empty square. Then select exactly one point each on three edges of the cell and connect them to form a new triangular cell (see Figure 6 (a)). This step generates a different fundamental table (Table 3) with the corresponding increments for the fundamental variables:  $\Delta F = 3, \Delta V = 3, \Delta N = 9$ . As before, the first three entries of the table express the fact that on each cell we have exactly one exponential clock, triggering the discrete step. It is noticeable that regardless of how many times this process is performed, it will result in only irregular nodes of nodal degree  $n^* = 3$ .





i	Name of step	$C_{i,0}$	$C_{i,1}$	$C_{i,2}$	$\lambda_i$	$\Delta N(i)$	$\Delta V(i)$	$\Delta F(i)$
3	Triangle crack	1	0	0	1	9	3	3

**Table 3.** The fundamental table of the micro event illustrated in Figure 6.

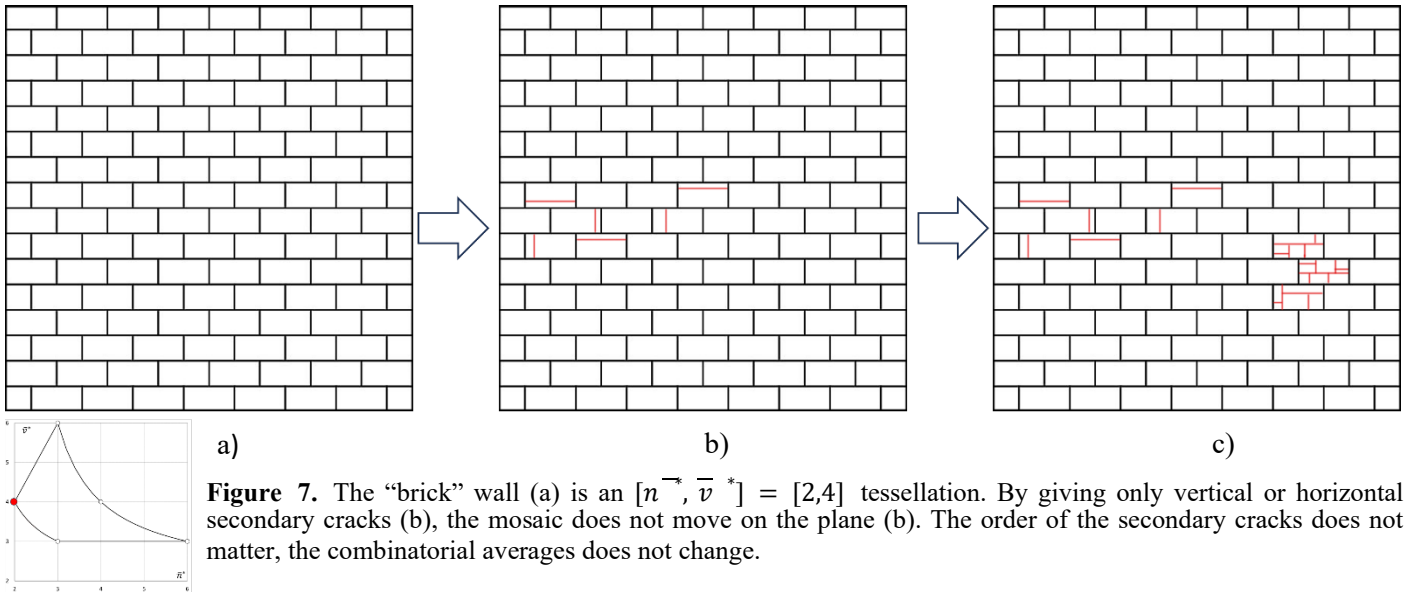
The algorithm described in article [6] allows us to define a model-specific version of the general differential equation system:

$$(7) \quad \frac{dx}{dt} = 3\lambda_0 y(1 - 3x)$$

$$(8) \quad \frac{dy}{dt} = 3\lambda_0 y(1 - 3y)$$

and we can see, we have  $x \rightarrow \frac{1}{3}$  and  $y \rightarrow \frac{1}{3}$  as  $t \rightarrow \infty$  which, via equations (3) and (4) also implies that  $\bar{n}^* \rightarrow 3$  and  $\bar{v}^* \rightarrow 3$  as  $t \rightarrow \infty$ .

**III.** Eventually, look at the (finite or not) orthogonal network a common brick wall gives us (see Figure 7 (a)). Since we can only see irregular nodes and rectangles the mosaic takes the  $[\bar{n}^*, \bar{v}^*] = [2,4]$  spot on the symbolic plane. If we only give (either horizontal or vertical) secondary cracks (see Figure 4) to the mosaic (see Figure 7 (b)) no other than irregular nodes and rectangular cells can be created. These are micro events, that occur after each other, and the order of which does not influence the combinatorial averages, only the visual appearance (see Figure 7 (c)).



**Remark.** In **III.** we inspected a special case of a Gilbert mosaic (see THE GILBERT-PIAFFE.), where we could operate with micro-events such as in [5] and [6].

## THE GILBERT-PIAFFE.

The Gilbert tessellation is a mathematical model that describes a specific type of convex mosaic formed by fractures. In this model, random points are set up on the plane, from which we then initiate fractures in two opposite directions at uniform speed along a direction defined by a randomly chosen angle until they reach another fracture resulting in a mosaic formed by irregular convex polygons (see Figure 8). It is noticeable that in all cases this process results in irregular nodes of type “T” with a nodal degree  $n^* = 2$ .

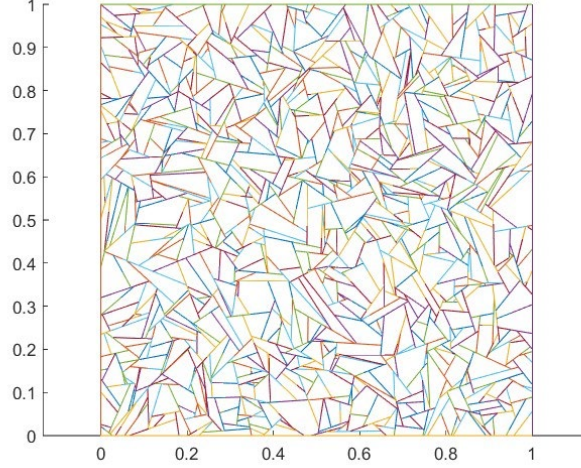


**Figure 8.** The Gilbert tessellation is a convex mosaic formed by irregular convex polygons having only irregular “T” nodes.

Using the mathematical knowledge presented previously, we can define a fundamental table that characterizes the evolution of this model (see Table 4.) Notice that a Gilbert tessellation is equivalent to a model where only secondary cracks occur.

i	Name of step	$C_{i,0}$	$C_{i,1}$	$C_{i,2}$	$\lambda_i$	$\Delta N(i)$	$\Delta V(i)$	$\Delta F(i)$
0	Straight crack	1	0	0	1	4	2	1

**Table 4.** The fundamental table for Gilbert tessellations.

It can be observed that the change in previously mentioned fundamental variables, which numerically describe the consequences of each step, in this specific case, will be:  $\Delta F = 1, \Delta V = 2, \Delta N = 4$ . As before, the first three entries of the fundamental table (Table 4) express the fact that on each cell we have exactly one exponential clock, triggering the discrete step.

The algorithm described in article [6] allows us to define a model-specific version of the general differential equation system:

$$(9) \quad \frac{dx}{dt} = 2\lambda_0 y(1 - 2x)$$

$$10 \quad \frac{dy}{dt} = \lambda_0 y(1 - 4y)$$

As it was shown in [6], in the flow defined by (9)-(10) we have  $x \rightarrow \frac{1}{2}$  and  $y \rightarrow \frac{1}{4}$  as  $t \rightarrow \infty$  which, via equations (3) and (4) also implies that  $\bar{n}^* \rightarrow 2$  and  $\bar{v}^* \rightarrow 4$  as  $t \rightarrow \infty$ . In other words, the mosaics following this model will end up in the *global attractor*  $(x_c, y_c) = \left(\frac{1}{2}, \frac{1}{4}\right)$  on the inverse symbolic plane, and in the global

attractor  $(\bar{n}^*, \bar{v}^*) = (2, 4)$  on the symbolic plane. Figure 9 illustrates the flow.

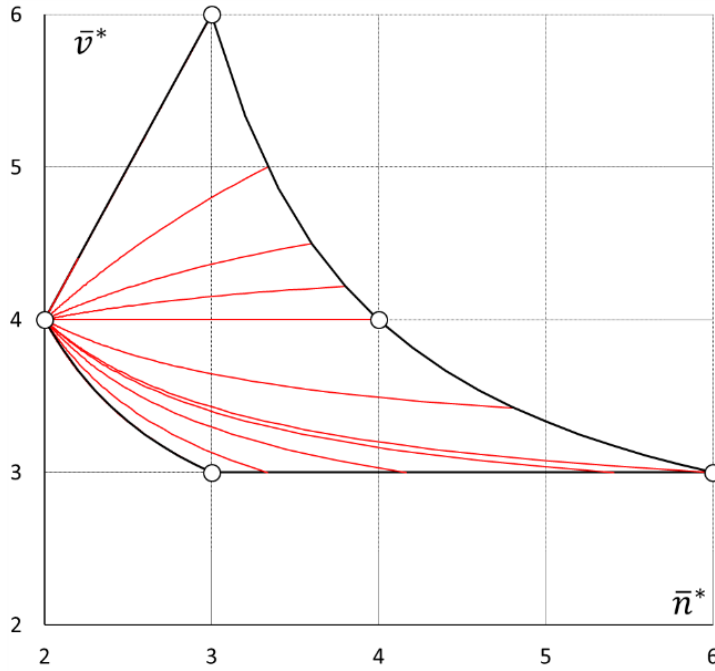


**Figure 9.** The mosaics following the Gilbert model end up in the  $[\bar{n}^*, \bar{v}^*] = [2, 4]$  on the symbolic plane.

As we can see, the flow (9)-(10) will carry any initial mosaic to the attractor at  $(\bar{n}^*, \bar{v}^*) = (2, 4)$ . However, if we consider an infinite Gilbert mosaic as initial condition, we notice that it is already located at that point. So the evolution of an infinite Gilbert mosaic under (5)-(6) is stationary process (in other words, a „piaffe”) on the symbolic plane, while the visible, geometric pattern will certainly evolve in time.

The theory presented in [6] applies, strictly speaking, only to infinite patterns, so the above argument about an *exact* „piaffe” where the symbolic point is *exactly* stationary only applies if the initial mosaic is infinite. However, all the arguments in [6] are based on limit processes where the size of the mosaic is approaching infinity, so we expect that the same model will deliver a fair approximation even if the initial mosaic is finite. In other words, we expect that if the initial model is finite then we will observe an *approximate* „piaffe” where the displacement of the symbolic point is scaling with some negative power of the size of the mosaic, i.e., as the size of the mosaic grows we expect the displacement of the symbolic point to decay. We will refer to this process as the *finite transient*.

Our main hypothesis is that the evolution of the combinatorial properties of the experiment presented earlier (see THE EXPERIMENT.) can be modelled by the evolution of the combinatorial properties of a suitably chosen Gilbert model. To verify our hypotheses, then, on one hand, we have to understand the behaviour of the infinite mosaic, on the other hand, we also have to describe the finite transient. The former task is provided by the adaptation of the analytical model of [6], for the second task we developed a numerical algorithm.

The most striking property observed when analysing the mosaic in the experiment is that it mostly consists of  $n^* = 2$ , “T” type irregular nodes. This fact is the basis for our hypothesis.

## NUMERICAL MODEL.

The theory of convex mosaics described earlier deals with infinite mosaics, but for a physical mosaic, such as in the experiment above, we have to take into account the differences due to its finite nature. Therefore, we have developed a numerical model based on the rules of the Gilbert mosaic but operating over a finite range.

In our model, we have introduced two additional free parameters that can be controlled to produce different versions of the general Gilbert mosaic. These two variables are:

1.  $P$ : the parameter defining the maximum deviation from the horizontal and the vertical directions, with range  $P > 4$ . The actual angle deviations will be computed as  $\Delta\alpha \in \left[-\frac{\pi}{P}, \frac{\pi}{P}\right]$ .
2.  $d$ : time delay between the initiation of each crack, where  $d \in [0,1]$

We constructed the simulation with the help of the program MATLAB. As the first step, we defined a unit square that will be the boundary of the mosaic, enclosing the mosaic in a finite frame. Then we picked  $M$  points  $p_i$ , ( $i=1,2, \dots M$ ) uniformly randomly within the square (see Figure 11(a)), where  $M$  is also a freely definable positive integer. The role of parameters from this point forward becomes evident in the algorithm.

In order to regulate the angles, we had to introduce parameter  $P$ . After picking the points  $p_i$ , we assigned a random angle  $\alpha = \alpha_0 + \Delta\alpha$ , where  $\alpha_0 \in \{0, \pi/2\}$ , and  $\Delta\alpha \in \left[-\frac{\pi}{P}, \frac{\pi}{P}\right]$ , by choosing uniformly randomly from both sets (see Figure 10). Note that the cracks start to grow from each point both in the assigned and in the opposite ( $2\pi - \alpha$ ) direction (see Figure 11(b)).

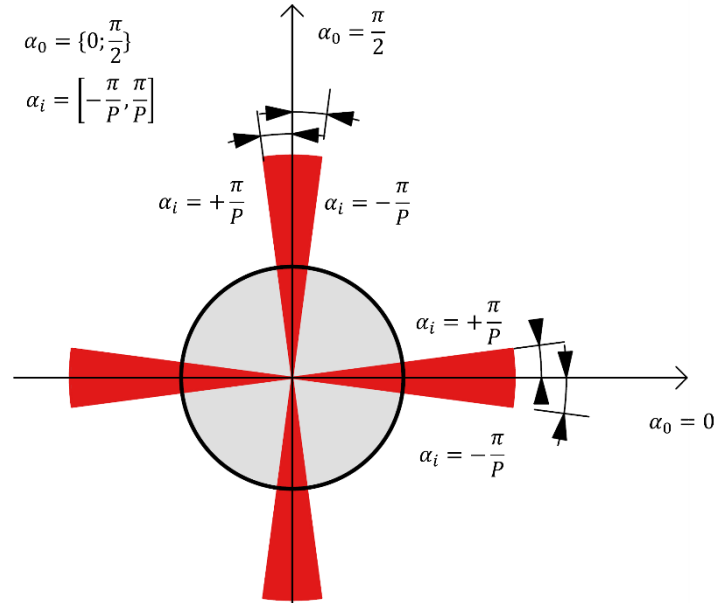


**Figure 10.** To produce a direction for the cracks we choose either the vertical ( $\alpha_0 = 0$ ) or horizontal ( $\alpha_0 = \frac{\pi}{2}$ ) axis and add a random  $\alpha_i$  to it regulated by the parameter  $P$ . Cracks start to grow in the randomly assigned and in the opposite direction.

By introducing parameter  $d$ , we can specify the time between the start of a crack and the start of the next crack. If  $d = 0$ , crack growth starts simultaneously from all points  $p_i$  ( $i=1, 2, \dots M$ ), and each crack stops when it reaches another one (or the edge of the unit square). At the other end of the interval,  $d = 1$ , when the time delay is the maximum, each fracture starts only when the previous one has fully finished developing. Even though the program operates with any  $\in [0,1]$ , for our results only the aforementioned two cases were used.

The first case ( $d = 0$ ) was implemented in the program with the following steps. We initially introduced a sufficiently small quantity called  $\Delta s$ , which represented the increase of a crack in one step. Afterwards, we took each of the points  $p_i$  listed in the matrix mentioned above one by one, drawing a segment of  $\Delta s$  length at the angle assigned to the points in both directions initiating the „fractures” this way. In the next step, we successively extended the existing tiny cracks by  $\Delta s$ , and so on, until one of the cracks intersected another segment (see Figure 11(c)) when we stored the data of the intersection and didn't extend that segment further on.

In the other scenario, where cracks develop consecutively ( $d = 1$ ), the difference will be that we extend the initial segment originating from the first point until it reaches the square forming the edge of the mosaic (see Figure 11(d)). Then the second crack will grow until it intersects with the other crack or the edge of the mosaic, the third until it meets the first two or the edges, and so on, until we have drawn a line from each point.

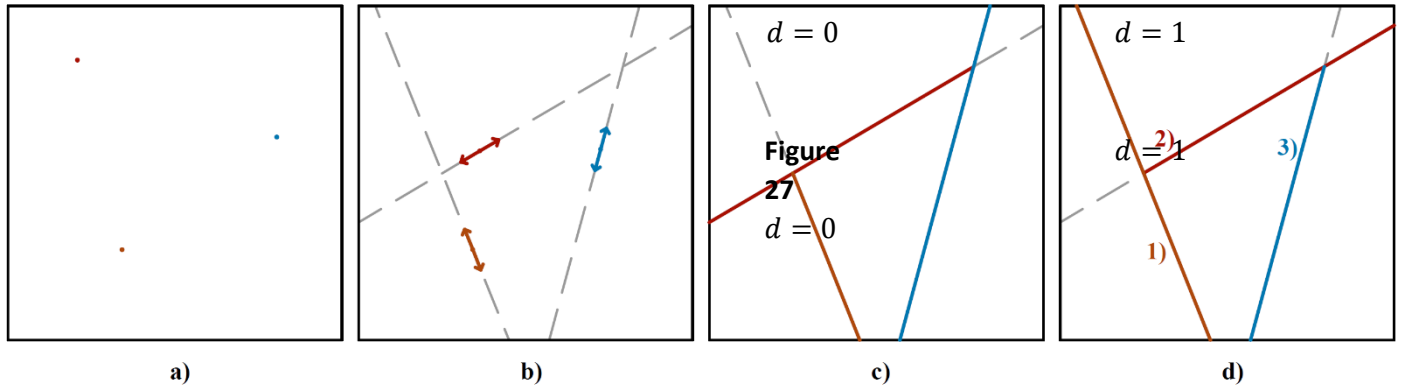


**Figure 11.** We pick  $M$  points  $p_i$  ( $i=1,2, \dots,M$ ) uniformly randomly within the unit square (a). We assign an angle to each point and the cracks start to grow in both directions (b). If  $d = 0$  we successively extend the existing tiny cracks until one of the cracks intersected another segment (c). If  $d = 1$  we extend the initial segment originating from the first point until it reaches the square forming the edge of the mosaic (d).

## RESULTS.

To test the validity of our hypothesis, we ran our simulation several times by varying the different parameters. Then we combinatorically analysed the temporal variation of the mosaics developed in the experiments and generated in the simulations by observing the temporal changes of the following values:

1.  $\bar{v}^*$ , the average cell degree

2.  $\sigma_{v^*}$ , the uncorrected standard deviation of the cell degree, defined as:  $\sigma_{v^*} = \sqrt{\frac{1}{N} \sum_{i=1}^N (v_i^* - \bar{v}^*)^2}$

The results indicated that it is more efficient to use the model where the parameter  $d$  is chosen as  $d = 1$ , meaning that in our simulations the cracks develop consecutively. At first, the angles associated with the starting points of the cracks were randomly chosen with uniform probability in the interval of  $\alpha \in [0, 2\pi]$ , corresponding to the case when  $P = 4$ . Using this model, the evolution of the average cell degree  $\bar{v}^*$  closely resembled the data measured in the experiment, however the time evolution of the standard deviation  $\sigma_{v^*}$  showed a significant difference from the experiment.

By varying the  $P$  parameter we obtained a simultaneous good match for both the average (see Figure 12) and the standard deviation (see Figure 13) at  $P=16$ .

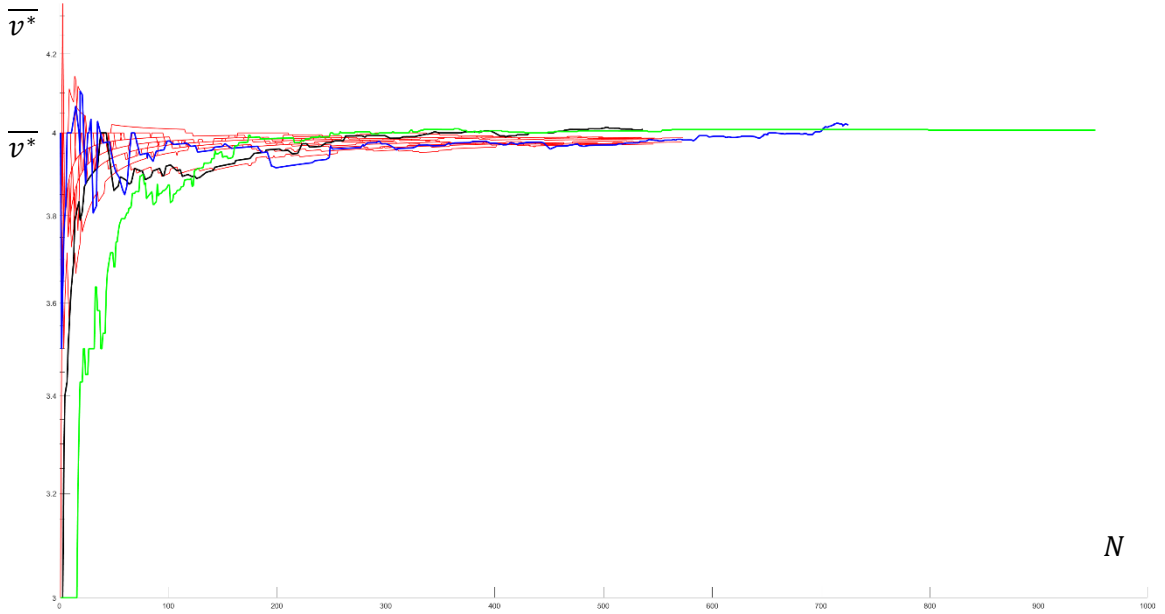


**Figure 12.** The average cell degree ( $\bar{v}^*$ ) as a function of the number of cells ( $N$ ). **Black: experiment nr. 1. Blue: experiment nr. 2. Green: Experiment nr. 3. Red: simulations.**  $N$

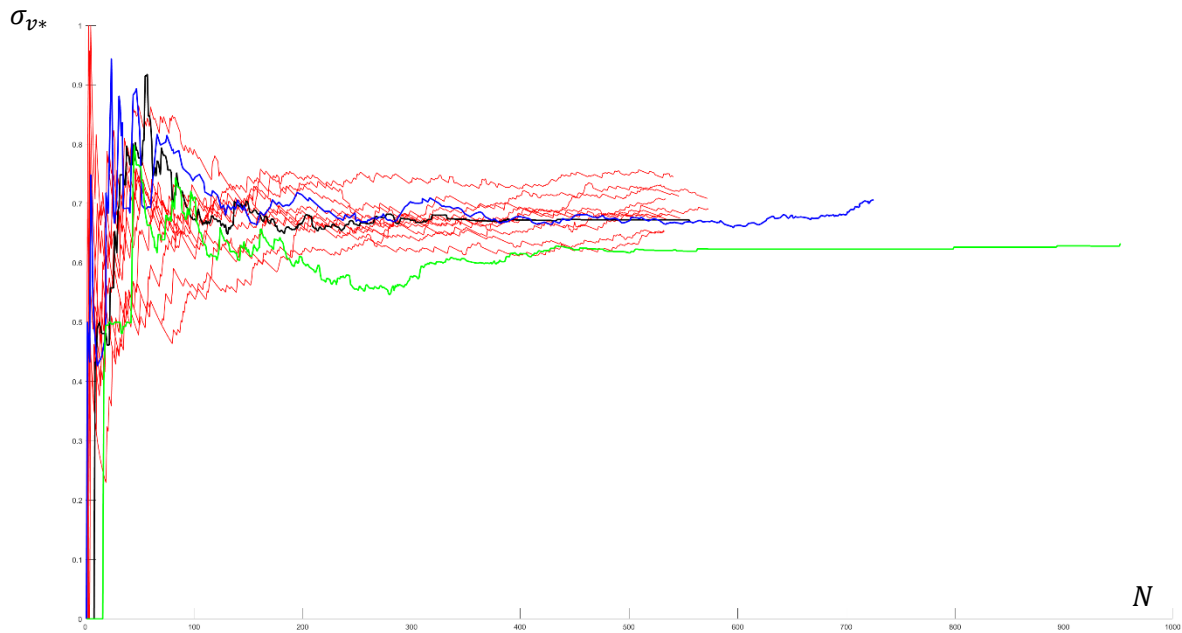


**Figure 13.** The uncorrected standard deviation of the cell degree  $\sigma_{v^*}$  as the function of the number of cells ( $N$ )  
**Black: experiment nr. 1. Blue: experiment nr. 2. Green: Experiment nr. 3. Red: simulations.**

The distribution of the cell degree  $v^*$  when the last cell is formed (in the last moment) is also of prime interest. Figure 14 illustrates that our model also captures the full distribution correctly.

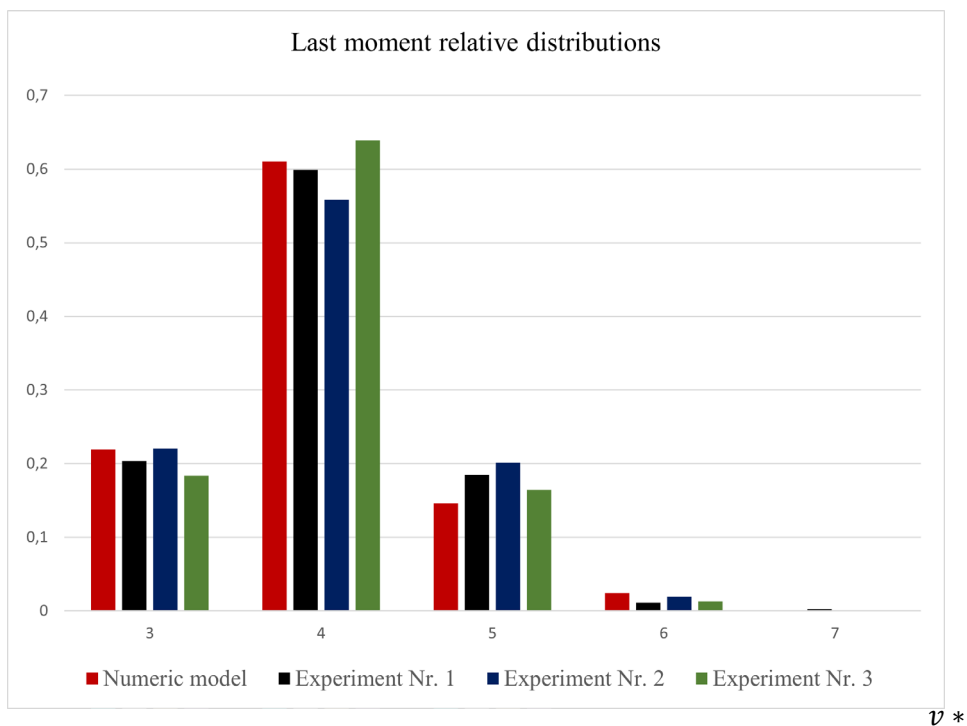


**Figure 14.** Relative distributions of the cell degrees when the last cell is formed of the experiment and a chosen numeric simulation.

**CONCLUSION.**

In our paper we first presented a well-documented series of experiments examining the temporal evolution of physical crack networks. Subsequently, we introduced mathematical tools from the theory of convex mosaics for the combinatorial analysis of crack networks. Given that this theory operates on infinite mosaics, we developed a numerical model which operates on a finite mosaic, and we implemented the evolution rules according to the rules of the Gilbert mosaic. By tuning the two model parameters (time delay  $d$  between cracks and angle deviation from orthogonal directions) we successfully achieved a simultaneous fit for the evolution of average, the evolution of the standard deviation as well as for the full distribution in the saturated phase.



- [1] A. Nakahara, et al., *Mechanism of memory effect of paste which dominates desiccation crack patterns*. Philosophical Transactions of the Royal Society A: Mathematical, Physical and Engineering Sciences, 377:20170395 (2019)
- [2] G. Domokos and Z. Lángi, *On some average properties of convex mosaics*. Experimental Mathematics, Vol. 31:3, pp. 783-793. (2022)
- [3] G. Domokos, Á.G. Horváth and K. Regős, *A two-vertex theorem for normal tilings.*, Aequationes Mathematicae, 97:185-197. (2023)
- [4] G. Domokos et.al. *Plato's cube and the natural geometry of fragmentation*. Proceedings of the National Academy of Sciences, 117(31), 18178–18185 (2020)
- [5] G. Domokos and K. Regős, *A discrete time evolution model for fracture networks*. Central European Journal of Operations Research. <https://doi.org/10.1007/s10100-022-00838-w> (2022).
- [6] P. Bálint, G. Domokos and K. Regős, *An Evolution Model for Polygonal Tessellations as Models for Crack Networks and Other Natural Patterns*. 8, Jul. 2023, Journal of Statistical Physics, 190, 130. <https://doi.org/10.1007/s10955-023-03146-y> (2023).

**TABLE OF FIGURES.**

Number of Figure:	Source:
1.	[1]
2.	[1]
3.	MS PowerPoint - self-made
4.	[6]
5.	Adobe PS 2021 – self-made
6.	Adobe PS 2021 – self-made
7.	Adobe PS 2021 – self-made
8.	MATLAB R2023a – self-made
9.	MS PowerPoint - self-made
10.	ArchiCad 26 – self-made
11.	ArchiCad 26 – self-made
12.	MATLAB R2023a – self-made
13.	MATLAB R2023a – self-made
14.	MS Excel – self-made

**ACKNOWLEDGEMENTS.**

Gergő Almádi and Eszter Ferencz kindly acknowledge support from the NKFIH Hungarian Research Fund grant 134199 and NKFIH grant TKP2021 BME-NVA, carried out at Budapest University of Technology and Economics. G.A. expresses his grateful appreciation of the gift representing the Albrecht Science Fellowship. G. A.'s research has been supported by the program UNKP-23-2 by ITM.